Ivo Senjanović
Smiljko Rudan
Nikola Vladimir

ISSN 1333-1124

INFLUENCE OF SHEAR ON THE TORSION OF THIN-WALLED GIRDERS

UDK 539.3:629.5

Summary

An improved theory of the torsion of thin-walled girders with open cross-section is presented. The influence of shear on torsion is taken into account. An analogy between shear-influenced bending and torsion is made. Application of the theory is illustrated in the case of a prismatic pontoon with a ship-like cross-section. The obtained results are verified by the 3D FEM analysis. It is shown that twist centre differs from the well-known shear centre.

Keywords: *thin-walled girders, torsion, warping, shear, analytical solution, FEM*

Nomenclature

A – cross-section area
A_i – integration constants
A_s – shear area
B – ship breadth
B_w – warping bimoment
E – Young's modulus
E_{tot} – strain energy
f – normal stress flow
G – shear modulus
g – shear stress flow
H – ship depth
I_b – cross-section moment of inertia
I_s – shear inertia modulus
I_t – torsional modulus
I_w – warping modulus
L – girder length
l – half of L, length of finite element
M – bending moment
M_t – external torque
Q – shear force
S_w – sectional moment of area portion
s – contour coordinate
T – torque
T_t – pure twist torque (St. Venant torque)
T_w – warping torque
t – plate thickness
S_w – sectional moment of area portion
u – axial displacement
w – deflection
w_b – bending deflection
w_s – shear deflection
$\bar{w}$ – warping function
x, y, z – Cartesian coordinate
β, γ – parameters
ϑ – twist deformation
μ_x – distributed torque
ν – Poisson's ratio
ξ – dimensionless coordinate
σ – normal stress
τ – shear stress
ψ – twist angle
ψ_s – shear twist angle
ψ_t – pure twist angle
$\mathbf{k}$ – stiffness matrix
$\boldsymbol{\mu}$ – load vector

1. Introduction

The influence of shear on the bending of a thin-walled girder is a well-known fact from Timoshenko's beam theory [1, 2, 3, 4]. The contribution of shear to beam deflection is increased with the aspect ratio of beam height and length. It is especially emphasized in the case of beam vibrations, where the distance between vibration nodes is relevant for the influence of shear. Thus, the influence of shear is increased for higher vibration modes [5].

In ordinary torsion theories of thin-walled girders with open cross-sections, the influence of shear on the twist angle is neglected [6, 7, 8, 9]. Therefore, the application of these theories is restricted to relatively long beams where the influence of shear can be ignored. However, that is not the case with relatively short girders such as ship hulls of large container ships [10, 11].

An advanced torsion theory of thin-walled girders, which takes the influence of shear into account, is presented in this paper. Following the analogy between bending and torsion, the shear effect is considered in similar way as in the case of bending [12, 13]. An analytical solution for a prismatic beam is given, and a beam finite element for non-uniform girders is developed for general use. The application of the numerical procedure is illustrated in the case of a prismatic pontoon with a ship-like cross-section. The obtained results are verified by the 3D FEM analysis.

2. Analogy between bending and torsion influenced by shear

Referring to Timoshenko's beam theory [1, 4, 14] one can assume that the total deflection, w, consists of pure bending deflection, w_b, and shear release, w_s, Fig. 1:

$$w = w_b + w_s \,, \tag{1}$$

where

$$w_s = -\frac{EI_b}{GA_s}\frac{\mathrm{d}^2 w_b}{\mathrm{d}x^2} \,. \tag{2}$$

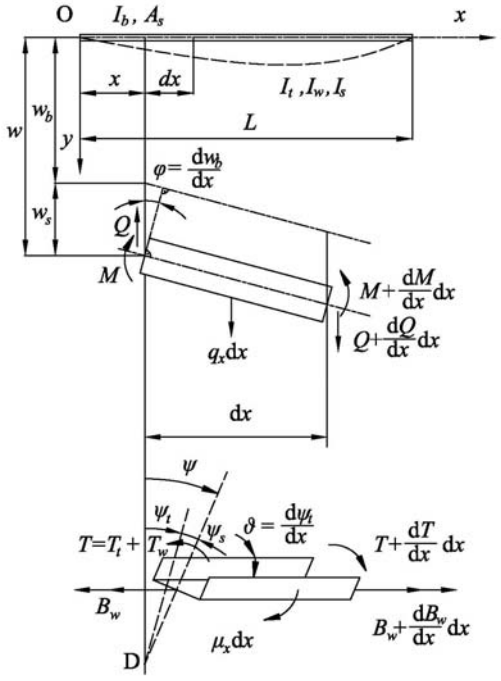

Fig. 1 Beam bending and torsion

E and G are the Young's and shear moduli, while I_b and A_s are the cross-section moment of inertia and the shear area, respectively. The angle of cross-section rotation is caused by the bending deflection

$$\varphi = \frac{\mathrm{d}\, w_b}{\mathrm{d}\, x}. \tag{3}$$

The sectional forces are the bending moment

$$M = -EI_b \frac{\mathrm{d}^2\, w_b}{\mathrm{d}\, x^2} \tag{4}$$

and the shear force

$$Q = GA_s \frac{\mathrm{d}\, w_s}{\mathrm{d}\, x} = -EI_b \frac{\mathrm{d}^3 w_b}{\mathrm{d}x^3}. \tag{5}$$

Similarly to bending, the total twist angle, ψ, consists of a pure twist angle, ψ_t, and the shear contribution, ψ_s, due to the effect of the shearing strain in the plane of the cross-section, Fig. 1 [4, 11].

$$\psi = \psi_t + \psi_s, \tag{6}$$

where

$$\psi_s = -\frac{EI_w}{GI_s} \frac{\mathrm{d}^2 \psi_t}{\mathrm{d}x^2}. \tag{7}$$

I_w and I_s are the warping modulus and the shear inertia modulus, respectively. The second beam displacement, which causes the warping of cross-section (analogous to the cross-section rotation due to bending), is a variation of pure twist angle

$$\vartheta = \frac{\mathrm{d}\psi_t}{\mathrm{d}x}. \tag{8}$$

The torsional sectional forces are the total torque, T, consisting of the pure twisting torque, T_t, and the warping torque, T_w, [4, 11], i.e.

$$T = T_t + T_w, \tag{9}$$

where

$$\begin{aligned} T_t &= GI_t \frac{\mathrm{d}\psi_t}{\mathrm{d}\, x} \\ T_w &= GI_s \frac{\mathrm{d}\psi_s}{\mathrm{d}x} = -EI_w \frac{\mathrm{d}^3 \psi_t}{\mathrm{d}\, x^3} \end{aligned} \tag{10}$$

and the warping (sectional) bimoment

$$B_w = EI_w \frac{\mathrm{d}^2 \psi_t}{\mathrm{d}x^2}. \tag{11}$$

I_t is the pure (St. Venant's) torsional modulus.

3. Definition of girder stiffness

Geometrical properties of a thin-walled girder include a cross-section area, A, moment of inertia of the cross-section and shear area in vertical and horizontal directions, I_b and A_s, respectively, torsional modulus I_t, warping modulus, I_w, and shear inertia modulus I_s. For a

simple cross-section these parameters can be determined analytically as pure geometrical properties [12, 13].

However, the determination of cross-section properties for an open multi-cell cross-section, as in the case of ship hull, is quite a difficult task. Therefore, the strip element method is applied for solving this statically undetermined problem [15]. First, the axial node displacements, due to bending caused by a shear force and due to torsion caused by a variation of twist angle, are calculated. Then, shear stress in bending τ_b, shear stress due to pure torsion τ_t, shear and normal stresses due to restrained warping τ_w and σ_w, respectively, are determined. Based on the equivalence of strain energies induced by sectional forces and calculated stresses, it is possible to formulate cross-section properties in the same way as given below:

shear area

$$A_s = \frac{Q^2}{\int\limits_A \tau_b^2 \mathrm{d}A} = \frac{1}{\int\limits_A g_b^2 \mathrm{d}A},\ g_b = \frac{\tau_b}{Q} \tag{12}$$

torsional modulus

$$I_t = \frac{T_t^2}{\int\limits_A \tau_t^2 \mathrm{d}A} = \frac{1}{\int\limits_A g_t^2 \mathrm{d}A},\ g_t = \frac{\tau_t}{T_t} \tag{13}$$

shear inertia modulus

$$I_s = \frac{T_w^2}{\int\limits_A \tau_w^2 \mathrm{d}A} = \frac{1}{\int\limits_A g_w^2 \mathrm{d}A},\ g_w = \frac{\tau_w}{T_w} \tag{14}$$

warping modulus

$$I_w = \frac{B_w^2}{\int\limits_A \sigma_w^2 \mathrm{d}A} = \frac{1}{\int\limits_A f_w^2 \mathrm{d}A},\ f_w = \frac{\sigma_w}{B_w} \tag{15}$$

The above quantities are not pure geometrical cross-section properties any more since they also depend on Poisson's ratio as a physical parameter.

4. Torsion of prismatic girder

Differential equation of the girder torsion represents the equilibrium between internal sectional torques, Eq. (9), and the external distributed torque, μ_x, [4, 16]

$$EI_w \frac{\mathrm{d}^4 \psi_t}{\mathrm{d}x^4} - GI_t \frac{\mathrm{d}^2 \psi_t}{\mathrm{d}x^2} = \mu_x . \tag{16}$$

The solution of the equation reads

$$\psi_t = A_0 + A_1 x + A_2 \mathrm{ch}\beta x + A_3 \mathrm{sh}\beta x + \psi_p , \tag{17}$$

where A_i are the integration constants,

$$\beta = \sqrt{\frac{GI_t}{EI_w}} \tag{18}$$

and ψ_p is a particular solution which depends on μ_x.

The total twist angle, according to (6), yields

$$\psi = A_0 + A_1 x + A_2\left(1-\frac{I_t}{I_s}\right)\mathrm{ch}\beta x + A_3\left(1-\frac{I_t}{I_s}\right)\mathrm{sh}\beta x + \psi_p - \frac{EI_w}{GI_s}\psi_p'' . \tag{19}$$

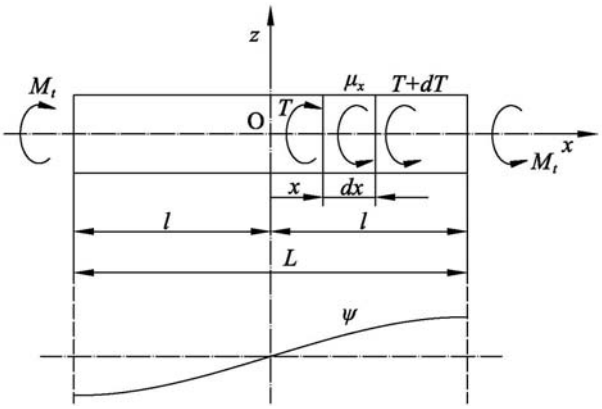

Fig. 2 Torsion of a free beam

As an illustrative example, let us consider the torsion of a girder loaded by a torque M_t at the ends, while $\mu_x = 0$, Fig. 2. The warping of the girder ends is restrained. In this case, the twist angle is an anti-symmetric function and therefore constants A_0 and A_2 in (19) are zero. The remaining constants A_1 and A_3 are determined by satisfying the boundary conditions

$$x = l: \qquad T = M_t, \qquad u = \frac{\mathrm{d}\psi_t}{\mathrm{d}x}\overline{w} = 0 , \tag{20}$$

where u is the function of axial displacements over cross-section, and $\overline{w}$ is the warping function (i.e. sectorial coordinate for a simple cross-section). Thus, one finds

$$A_1 = \frac{M_t}{GI_t}, \; A_3 = -\frac{M_t}{GI_t\beta\mathrm{ch}\beta l} \tag{21}$$

and displacements and sectional forces take the following form:

total twist angle

$$\psi = \frac{M_t l}{GI_t}\left[\frac{x}{l} - \left(1-\frac{I_t}{I_s}\right)\frac{\mathrm{sh}\beta x}{\beta l\mathrm{ch}\beta l}\right] \tag{22}$$

axial displacement due to warping

$$u = \frac{M_t}{GI_t}\left(1-\frac{\mathrm{ch}\beta x}{\mathrm{ch}\beta l}\right)\overline{w} \tag{23}$$

pure twisting and warping torques

$$T_t = M_t\left(1-\frac{\mathrm{ch}\beta x}{\mathrm{ch}\beta l}\right), \; T_w = M_t\frac{\mathrm{ch}\beta x}{\mathrm{ch}\beta l} \tag{24}$$

warping bimoment

$$B_w = -M_t\frac{\mathrm{sh}\beta x}{\beta\mathrm{ch}\beta l} . \tag{25}$$

Total torque $T = T_t + T_w = M_t$ is uniform along the beam.

5. Beam finite element

One of the most efficient ways to solve torsion of a non-uniform girder is the application of the finite element method. The beam finite element properties can be derived by the energy approach. The strain energy reads [14]

$$E_{tot} = \frac{1}{2}\int_0^l \left[EI_w \left(\frac{\mathrm{d}^2 \psi_t}{\mathrm{d}x^2} \right)^2 + GI_s \left(\frac{\mathrm{d}\psi_s}{\mathrm{d}x} \right)^2 + GI_t \left(\frac{\mathrm{d}\psi_t}{\mathrm{d}x} \right)^2 \right] \mathrm{d}x - \\ - \int_0^l \mu\psi \mathrm{d}x + (T\psi + B_w\vartheta)_0^l , \tag{26}$$

where l is the element length. A two-node finite element has four torsional degrees of freedom, Fig. 3,

$$\mathbf{V} = \begin{Bmatrix} \psi(0) \\ \vartheta(0) \\ \psi(l) \\ \vartheta(l) \end{Bmatrix}. \tag{27}$$

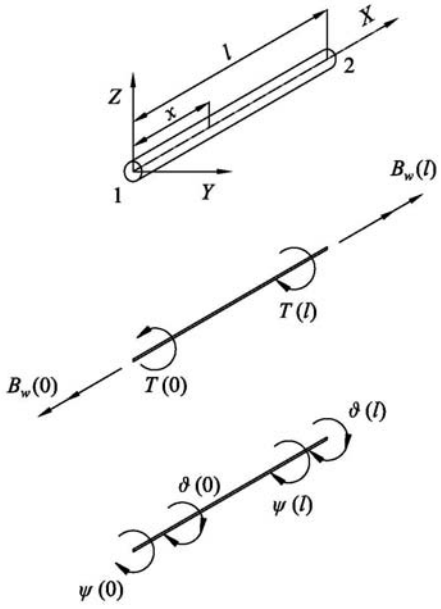

Fig. 3 Beam finite element

The basic beam displacement ψ_t can be presented by a third-order polynomial

$$\psi_t = \langle d_k \rangle \xi^k, \; k = 0,1,2,3 \\ \xi = \frac{x}{l}, \; \langle \dots \rangle = \{ \dots \}^T . \tag{28}$$

Furthermore, by satisfying alternately the unit value for one of the nodal displacements **V** and zero values for the remaining displacements, it follows that

$$\psi_t = \langle \psi_{ti} \rangle \mathbf{V}, \; \psi_s = \langle \psi_{si} \rangle \mathbf{V}, \; \psi = \langle \psi_i \rangle \mathbf{V}, \; i = 1,2,3,4, \tag{29}$$

where ψ_{ti}, ψ_{si}, and ψ_i are the following shape functions:

$$\psi_{ti} = \langle d_{ik} \rangle \xi^k, \; \psi_{si} = \langle e_{ik} \rangle \xi^k, \; \psi_i = \langle f_{ik} \rangle \xi^k \tag{30}$$

$$\mathbf{d}_{ik} = \frac{1}{1+12\gamma}\begin{bmatrix} 1+6\gamma & 0 & -3 & 2 \\ -4\gamma(1+3\gamma)l & (1+12\gamma)l & -2(1+3\gamma)l & l \\ 6\gamma & 0 & 3 & -2 \\ -2\gamma(1-6\gamma)l & 0 & -(1-6\gamma)l & l \end{bmatrix} \tag{31}$$

$$\mathbf{e}_{ik} = \frac{1}{1+12\gamma}\begin{bmatrix} 6\gamma & -12\gamma & 0 & 0 \\ 4\gamma(1+3\gamma)l & -6\gamma l & 0 & 0 \\ -6\gamma & 12\gamma & 0 & 0 \\ 2\gamma(1-6\gamma)l & -6\gamma l & 0 & 0 \end{bmatrix} \tag{32}$$

$$\mathbf{f}_{ik} = \mathbf{d}_{ik} + \mathbf{e}_{ik}\ , \quad \gamma = \frac{EI_w}{GI_s l^2}\,. \tag{33}$$

By substituting (29) into (26), one obtains

$$E_{tot} = \frac{1}{2}\mathbf{V}^T\left[\mathbf{k}_{ws} + \mathbf{k}_t\right]\mathbf{V} - \langle\mu\rangle\mathbf{V} - \langle R\rangle\mathbf{V}\,, \tag{34}$$

where, assuming constant values of the element properties,

$$\mathbf{k}_{ws} = \left[EI_w \int_0^l \frac{\mathrm{d}^2\psi_{ti}}{\mathrm{d}x^2}\frac{\mathrm{d}^2\psi_{tj}}{\mathrm{d}x^2}\mathrm{d}x + GI_s\int_0^l \frac{\mathrm{d}\psi_{si}}{\mathrm{d}x}\frac{\mathrm{d}\psi_{sj}}{\mathrm{d}x}\mathrm{d}x \right] \tag{35}$$

is the warping-shear stiffness matrix,

$$\mathbf{k}_t = \left[GI_t \int_0^l \frac{\mathrm{d}\psi_{ti}}{\mathrm{d}x}\frac{\mathrm{d}\psi_{tj}}{\mathrm{d}x}\mathrm{d}x \right] \tag{36}$$

is the torsional stiffness matrix,

$$\boldsymbol{\mu} = \left\{ \int_0^l \mu\psi_j\,\mathrm{d}x \right\}, \qquad i,j = 1,2,3,4 \tag{37}$$

is the torsional load vector and

$$\mathbf{R} = \begin{Bmatrix} -T(0) \\ -B_w(0) \\ T(l) \\ B_w(l) \end{Bmatrix} \tag{38}$$

is the nodal force vector. Furthermore, by taking Eq. (30) into account, the stiffness matrices, Eqs (35) and (36), are developed to their final forms:

$$\mathbf{k}_{ws} = \frac{2EI_w}{(1+12\gamma)l^3}\begin{bmatrix} 6 & 3l & -6 & 3l \\ & 2(1+3\gamma)l^2 & -3l & (1-6\gamma)l^2 \\ & & 6 & -3l \\ Sym. & & & 2(1+3\gamma)l^2 \end{bmatrix} \tag{39}$$

$$\mathbf{k}_t = \frac{GI_t}{30(1+12\gamma)^2 l}\begin{bmatrix} 36 & 3(1-60\gamma)l & -36 & 3(1-60\gamma)l \\ & 4(1+15\gamma+360\gamma^2)l^2 & -3(1-60\gamma)l & -(1+60\gamma-720\gamma^2)l^2 \\ & & 36 & -3(1-60\gamma)l \\ Sym. & & & 4(1+15\gamma+360\gamma^2)l^2 \end{bmatrix} \tag{40}$$

For linearly distributed load along the finite element

$$\mu = \mu_0 + \mu_1 \xi \tag{41}$$

the load vector (37) reads

$$\boldsymbol{\mu} = \frac{\mu_0 l}{12}\begin{Bmatrix} 6 \\ l \\ 6 \\ -l \end{Bmatrix} + \frac{\mu_1 l}{60(1+12\gamma)}\begin{Bmatrix} 9+120\gamma \\ (2+30\gamma)l \\ 21+240\gamma \\ -(3+30\gamma)l \end{Bmatrix}. \tag{42}$$

It should be mentioned that the constitution and construction of torsional properties for the beam finite element are very similar to bending properties since the same shape functions are used in both cases [14].

The total element energy has to be at its minimum, and by satisfying the relevant condition

$$\frac{\partial E_{tot}}{\partial \mathbf{V}} = \mathbf{0}, \tag{43}$$

the ordinary form of the finite element equation is obtained

$$\mathbf{R} = (\mathbf{k}_{ws} + \mathbf{k}_t)\mathbf{V} - \boldsymbol{\mu}. \tag{44}$$

6. Torsion of ship-like pontoon

A uniform pontoon of a double skin open cross-section of a 7800 TEU (Twenty-feet Equivalent Units) container ship is considered, Fig. 4. The pontoon length is $L = 2l = 300$ m. According to the program STIFF [17], based on the thin-walled girder theory [15], the cross-section properties are determined as follows:

cross-section area	A = 6.394 m^2
horizontal shear area	A_{sh} = 1.015 m^2
vertical shear area	A_{sv} = 1.314 m^2
vertical position of neutral line	z_{NL} = 11.66 m
vertical position of shear centre	z_{SC} = -13.50 m
horizontal moment of inertia	I_{bh} = 1899 m^4
vertical moment of inertia	I_{bv} = 676 m^4
torsional modulus	I_t = 14.45 m^4
shear inertia modulus	I_s = 710.5 m^4
warping modulus	I_w = 171400 m^6.

Young's modulus, shear modulus and Poisson's ratio are $E = 2.06\text{x}10^8$ kN/m^2, $G = 0.7923\text{x}10^8$ kN/m^2, $\nu = 0.3$, respectively. The position of shear centre, z_{SC}, is rather low due to the open cross-section. The warping function of cross-section, $\bar{w}$, is shown in Fig. 5. The shear stress flows, g_t and g_w, and the normal stress flow, f_w, are shown in Figs. 6, 7 and 8, respectively. Distribution of f_w over the cross-section according to (20) is the same as $\bar{w}$ [4].

$$\sigma = \frac{\partial u}{\partial x} = \frac{\mathrm{d}^2 \psi_t}{\mathrm{d}x^2}\bar{w}. \tag{45}$$

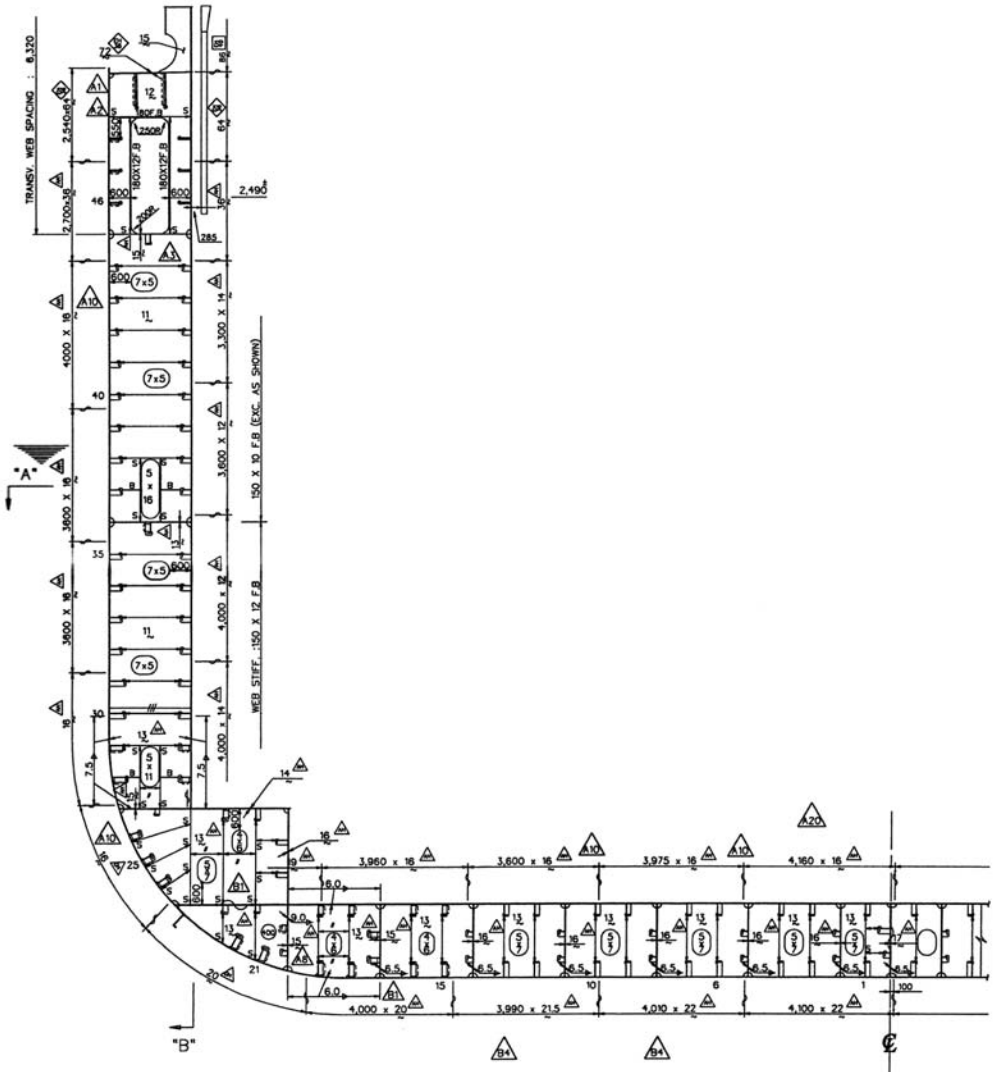

Fig. 4 Midship cross-section of a container ship

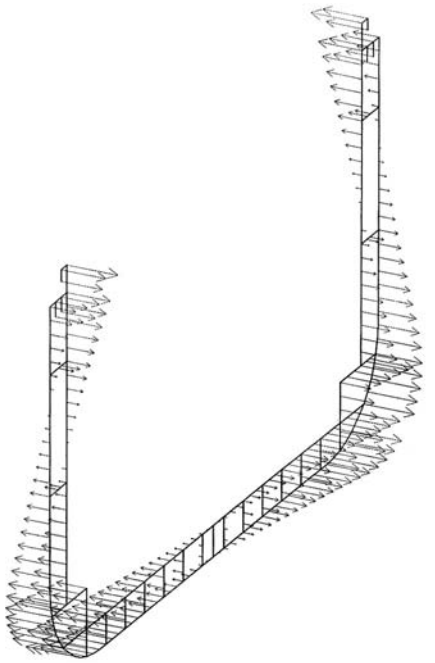

Fig. 5 Warping function of cross-section

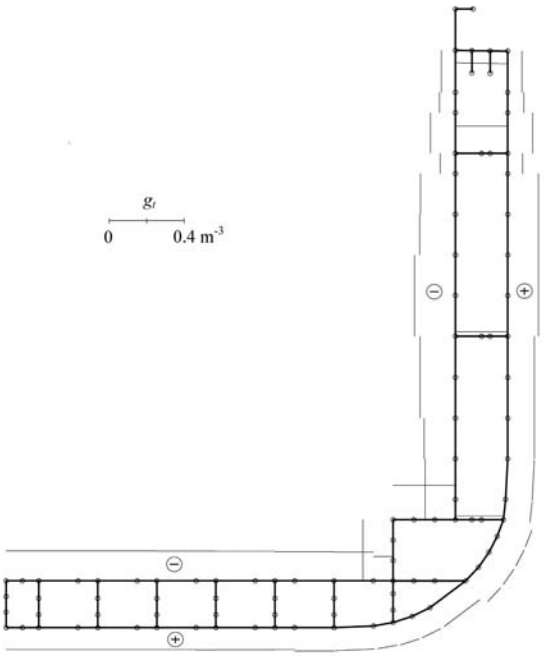

Fig. 6 Shear stress flow due to torsion

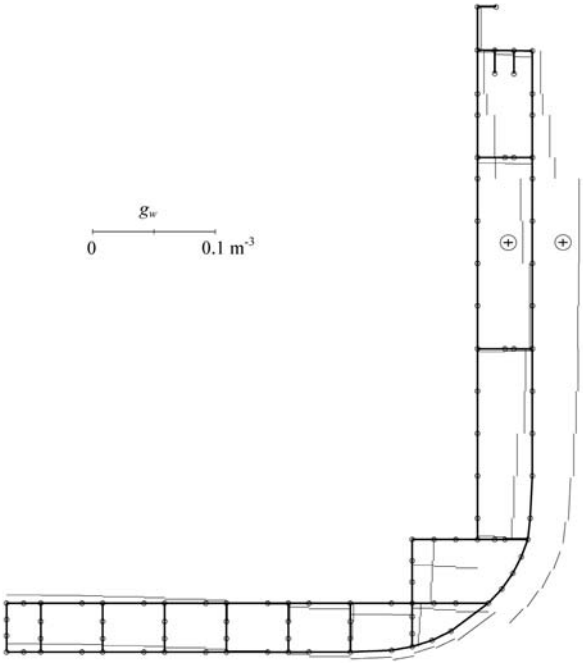

Fig. 7 Shear stress flow due to restrained warping

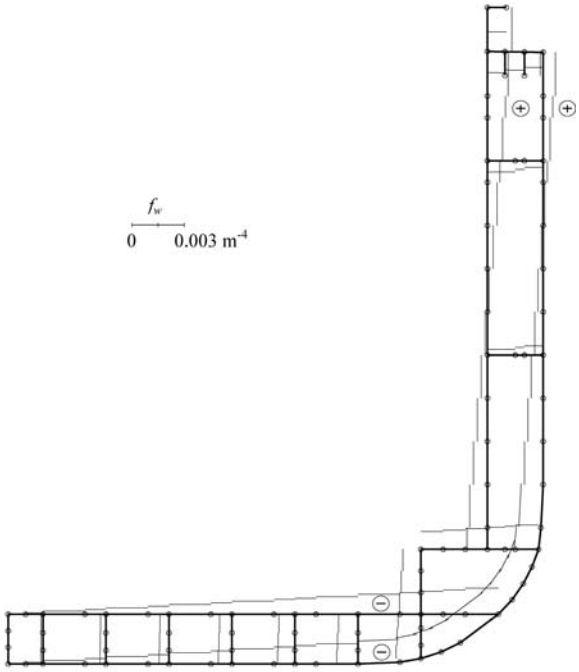

Fig. 8 Normal stress flow due to restrained warping

The pontoon is loaded by torques $M_t = \pm 40570$ kNm at its ends, Fig. 2. Warping of the pontoon ends is restrained; therefore, the formulae for displacements and sectional forces derived in Section 4 are relevant. Diagram of twist angle, ψ, with indicated shear contribution, ψ_s, in dimensionless form, is shown in Fig. 9. Longitudinal distribution of the relative axial (warping) displacement, $u/\bar{w}$, is shown in Fig. 10. Twisting and warping torques, T_t and T_w, which equilibrate together the constant load M_t, are presented in Fig. 11. Fig. 12 shows the distribution of warping bimoment, B_w, as a result of the normal stress distribution over cross-section.

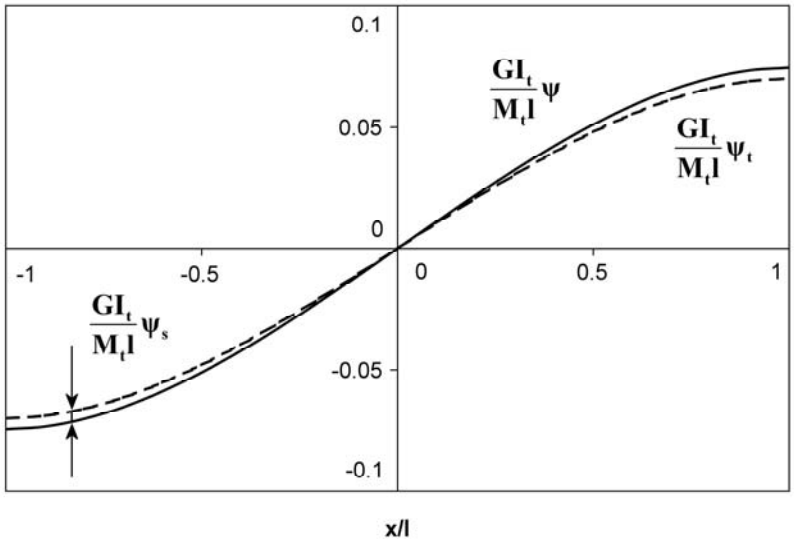

Fig. 9 Pontoon twist angle

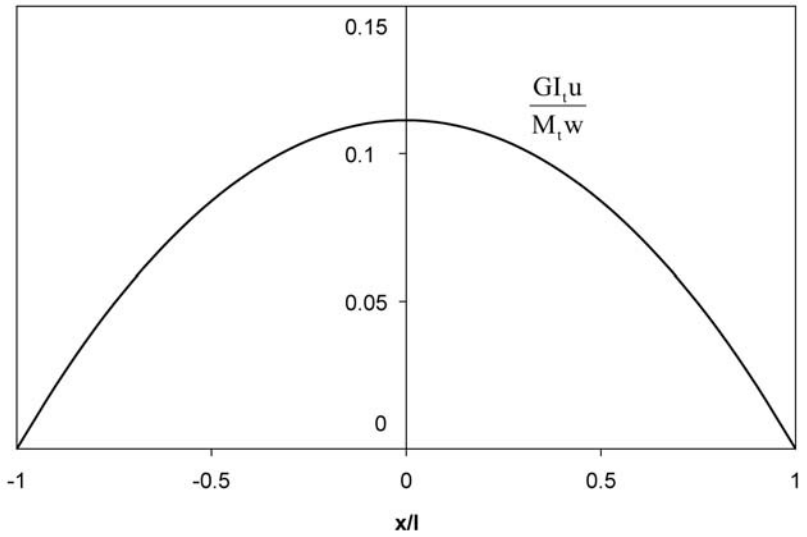

Fig. 10 Relative axial displacement

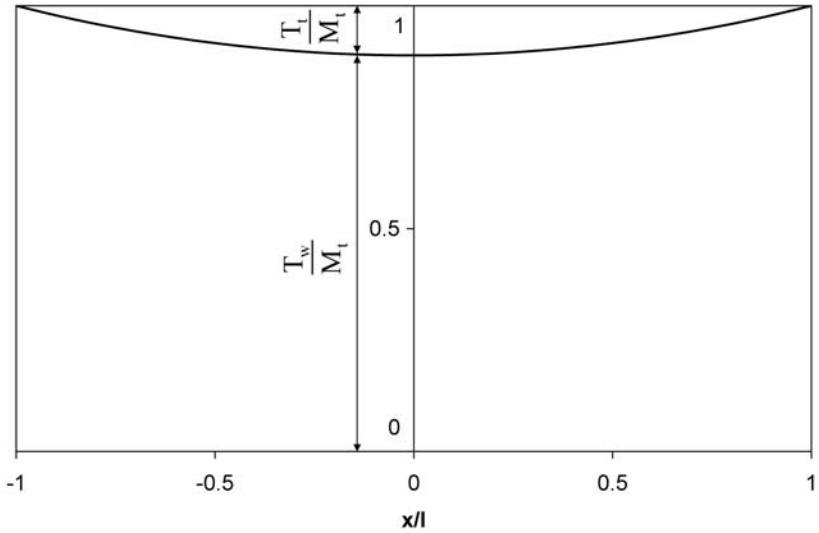

Fig. 11 Twisting and warping torques

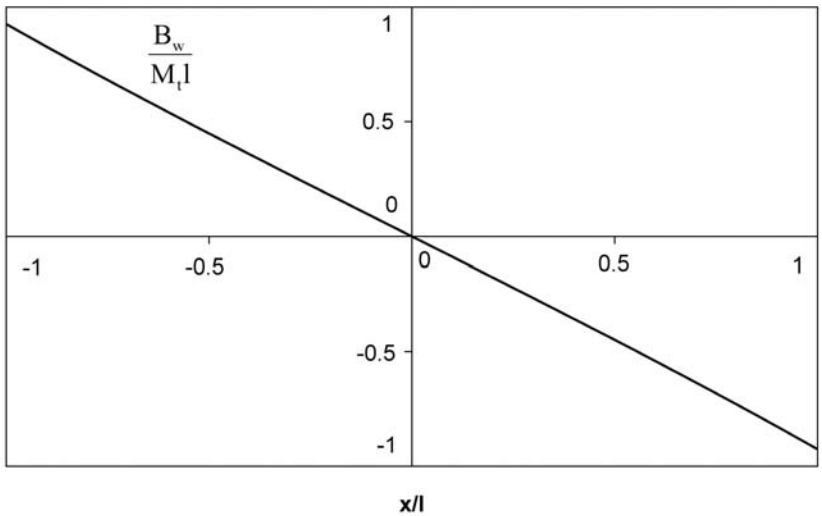

Fig. 12 Warping bimoment

7. Verification of a beam model

The pontoon strength analysis is performed by combining the beam theory with the thin-walled girder theory for determining beam cross-section properties. The reliability of such a combined (1+2)D model is checked by a comparison with the results of 3D FEM analysis, performed by means of software [18].

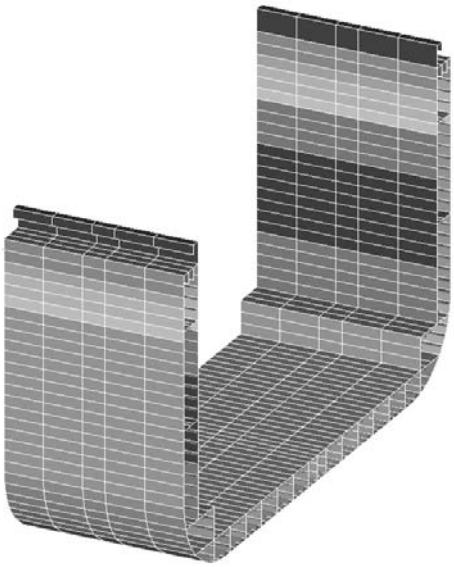

Fig. 13 A typical pontoon superelement

The pontoon structure is represented by 22 superelements. A typical superelement, consisting of shell finite elements, is shown in Fig. 13. The pontoon ends are closed with transverse bulkheads. The pontoon is loaded at its ends with forces on the left and the right side of each end distributed vertically in the opposite directions. In this way these forces generate the total torque $M_t = 40570$ kNm, Fig. 14. Transverse and vertical displacements are fixed in the midship section, and axial displacements (warping) are fixed at the pontoon ends.

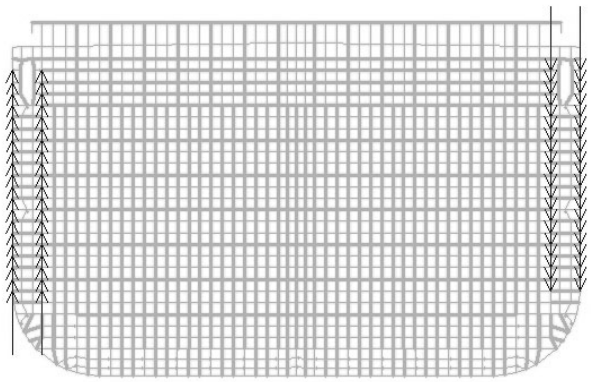

Fig. 14 Load at the model free end

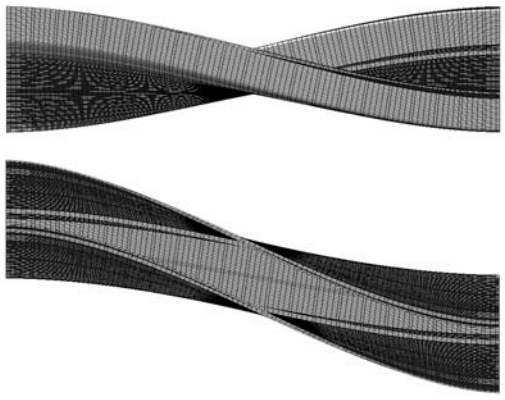

Fig. 15 Lateral and bird's-eye views of a deformed pontoon

The lateral and bird's-eye views of the deformed pontoon model are shown in Fig. 15. The distortion of the pontoon cross-section is not noticed since the double skin is reinforced with rather rigid web frames, Fig. 4. For the same reason, bending stresses in the plating are negligible compared to membrane stresses; therefore, the structure behaves as a membrane one. Since these assumptions introduced in the thin-walled girder theory are satisfied, the obtained results of the 3D FEM analysis are comparable to those of the (1+2)D model.

If one draws a twist angle diagram based on 3D FEM results, he would obtain the same shape as that from the (1+2)D analysis, Fig. 9. The ratios of the maximum displacements in two models, i.e. their twist angles and warping displacements, read

$$x = L/2: \ \frac{\psi_{(1+2)\mathrm{D}}}{\psi_{3\mathrm{D}}} = \frac{0.00108934}{0.00108192} = 1.00685,$$

$$x = 0, \text{ upper deck: } \frac{u_{(1+2)\mathrm{D}}}{u_{3\mathrm{D}}} = \frac{-2.18718}{-2.17655} = 1.00488,$$

$$x = 0, \text{ bilge: } \frac{u_{(1+2)\mathrm{D}}}{u_{3\mathrm{D}}} = \frac{2.63947 \text{ mm}}{2.59264 \text{ mm}} = 1.01806.$$

The discrepancies of displacements are within 2%, which is quite good.

The maximum twist angles at the pontoon ends are also compared in Fig. 16. The total twist angle of the analytical solution, $\psi_{(1+2)\mathrm{D}}$, is almost equal to that of the FEM analysis, $\psi_{3\mathrm{D}}$. The value of $\psi_{(1+2)\mathrm{D}}$ consists of a pure torsional part ψ_t and shear contribution ψ_s. The former causes the cross-section rotation around the shear centre, S.C., while the additional rotation by the latter one is realized around the section of the double bottom neutral line and the cross-section centreline, point P in Fig. 16. As a result, the twist centre, T.C., which slightly differs from the shear centre, S.C., is defined.

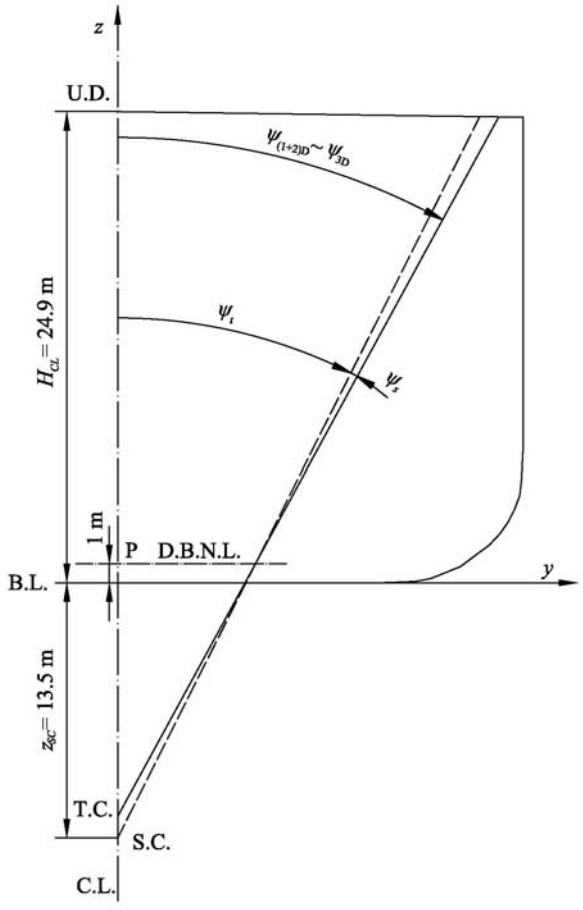

Fig. 16 Twist angle at the pontoon end

8. Conclusion

The ordinary torsional theory of thin-walled girders is extended by taking into account the influence of shear on the cross-section rotation. The analogy between the shear-influenced bending and torsion is emphasized. The shear inertia modulus is specified as a result of shear flow due to restrained warping. In the analytical solution of uniform beam torsion an explicit insight into the role of all relevant geometrical parameters is possible. The theory is verified by the correlation analysis of the analytical solution for a pontoon with a ship-like cross-section and of the 3D FEM solution. Quite good agreement between the results is obtained. The analysis shows that the shear centre in the thin-walled girder theory is also the twist centre if the influence of shear on torsion is neglected. However, the shear effect slightly changes the position of the twist centre, as it is confirmed by the 3D FEM analysis. Pure twist rotation due St. Venant's torsion is realised around the shear centre. On the other hand, as a novelty, the rotational centre for additional cross-section angle due to the shear effect lies on the neutral line of the centreline longitudinal section. The described theory and the numerical example taken from the naval architecture practice show the importance of incorporating the shear effect into the torsion analysis of large container ships, which are relatively flexible due to large hatch openings [19].

ACKNOWLEDGMENTS

This research was supported by the Ministry of Science, Education and Sport of the Republic of Croatia (Project No. 120-1201703-1704).

APPENDIX: SHEAR INERTIA MODULUS OF A U-GIRDER

The open midship cross-section of the ship hull can be approximately idealized with a U-section, Fig. A1. In that case the cross-section properties can be determined analytically. According to [4, 11, 12], the shear inertia modulus is presented in the following form:

$$I_s = \frac{I_w^2}{\int_A \left(\frac{S_w^*}{t} \right) \mathrm{d}A}, \tag{A1}$$

where S_w^* is the sectorial moment of the cut-off portion of the cross-section area, and A is the total area.

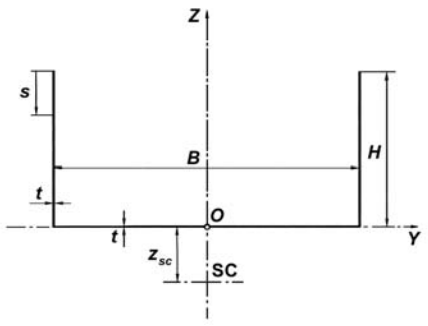

Fig. A1 Idealized ship cross-section

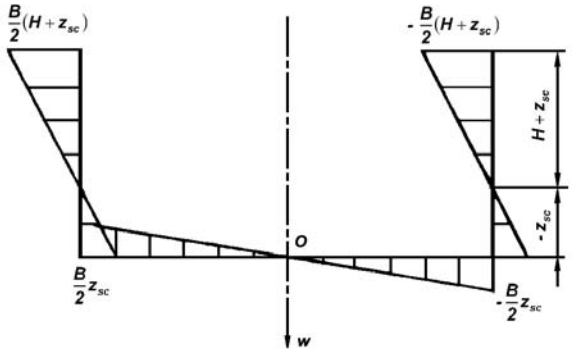

Fig. A2 Sectional coordinate, $\overline{w}$

Referring to [11], the sectorial coordinate for the side shell and bottom, Fig. A2, read:

$$w_1 = \frac{B}{2}\left(H + z_{SC} - s\right), \qquad 0 < s < H, \tag{A2}$$

$$w_2 = z_{SC}\left(H + \frac{B}{2} - s\right), \qquad H < s < H + B, \tag{A3}$$

where

$$z_{SC} = -\frac{3H^2}{B + 6H} \tag{A4}$$

is the coordinate of the shear centre, Fig. A1. The warping modulus, according to definition, yields

$$I_w = \int_A w^2 \mathrm{d}A = \frac{B^2 t}{6}\left[\left(H + z_{SC}\right)^3 + \left(\frac{B}{2} - z_{SC}\right) z_{SC}^2\right]. \tag{A5}$$

The sectorial moment is split into two domains, Fig. A3:

$$S_{w1}^* = \int_0^s w_1 t \mathrm{d}s = \frac{Bt}{2}\left[\left(H + z_{SC}\right)s - \frac{s^2}{2}\right], \qquad 0 < s < H, \tag{A6}$$

$$\begin{aligned} S_{w2}^* &= S_{w1}^*\Big|_0^H + \int_H^s w_2 t \mathrm{d}s \\ &= \frac{BtH^2}{4} + z_{SC} t\left[-\frac{H^2}{2} + \left(H + \frac{B}{2}\right)s - \frac{s^2}{2}\right], \qquad H < s < H + B. \end{aligned} \tag{A7}$$

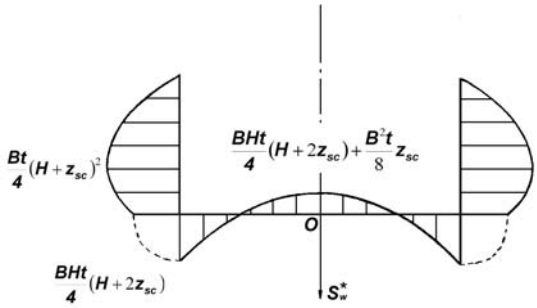

Fig. A3 Integral of a sectional coordinate, S_w^*

One finds for the integrals of shear flow that

$$I_{f1} = 2\int_0^H \left(\frac{S_{w1}^*}{t}\right)^2 t\mathrm{d}s = \frac{B^2 t H^3}{120}\left(8H^2 + 25Hz_{SC} + 20z_{SC}^2\right) \tag{A8}$$

$$\begin{aligned} I_{f2} &= 2\int_H^{H+\frac{B}{2}} \left(\frac{S_{w2}^*}{t}\right)^2 t\mathrm{d}s \\ &= \frac{B^3 t}{240}\left[15H^4 + 10H^2\left(B+6H\right)z_{SC} + 2\left(B^2 + 10HB + 30H^2\right)z_{SC}^2\right]. \end{aligned} \tag{A9}$$

REFERENCES

[1] Timoshenko S, Young DH. Vibration problems in engineering. D Van Nostrand, 1955.

[2] Cowper GR. The shear coefficient in Timoshenko's beam theory. Journal of Applied Mechanics 1966;33:335-40.

[3] Senjanović I, Fan Y. The bending and shear coefficients of thin-walled girders. Thin-Walled Structures 1990;10:31-57.

[4] Pavazza, R. Introduction to thin-walled beam analysis. Kigen, Zagreb, 2007. (in Croatian).

[5] Senjanović I, Fan Y. A higher-order theory of thin-walled girders with application to ship structures. Computers and Structures Vol. 43, No. 1, pp. 31-52, 1992.

[6] Vlasov VZ. Thin-walled elastic beams. Jerusalem: Israel Program for Scientific Translation Ltd.; 1961.

[7] Kollbruner CF, Basler K. Torsion in structures. Berlin: Springer; 1969.

[8] Gjelsvik A. The theory of thin-walled bars. New York: Wiley; 1981.

[9] Haslum K, Tonnessen A. An analysis of torsion in ship hull. European Shipbuilding 1972;5/6:67-89.

[10] Pedersen PT. Torsional response of containerships. Journal of Ship Research 1985;29:194-205.

[11] Senjanović I, Tomašević S, Rudan S, Senjanović T. Role of transverse bulkheads in hull stiffness of large container shops. Engineering Structures 2008;30:2492-2509.

[12] Pavazza R. Bending and torsion of thin-walled beams of open cross-section on elastic foundation. PhD thesis, Faculty of Mechanical Engineering and Naval Architecture, University of Zagreb, Zagreb; 1991.

[13] Pavazza R. Torsion of thin-walled beams of open cross-section with influence of shear. International Journal of Mechanical Sciences 2005;47:1099-1122.

[14] Senjanović I, Grubišić R. Coupled horizontal and torsional vibration of a ship hull with large hatch openings. Computers and Structures, Vol. 41, No. 2, pp. 213-226, 1991.

[15] Senjanović I, Fan Y. A finite element formulation of ship cross-sectional stiffness parameters. Brodogradnja 1993;41:27-36.

[16] Senjanović I, Fan Y. Pontoon torsional strength analysis related to ships with large deck openings. Journal of Ship Research, Vol. 35, No. 4, Dec. 1991, pp. 339-351.

[17] Fan Y, Senjanović I. STIFF. User's manual. FAMENA, Zagreb; 1990.

[18] Det Norske Veritas. SESAM. User's manual. Høvik; 2007.

[19] Senjanović I, Tomašević S, Rudan S, Tomić, M, Vladimir N, Malenica Š. Hydroelasticity of very large container ships. Proceedings of Design and Operation of Container Ships. RINA, London, 2008.

Submitted: 30.01.2009

Accepted: 05.6.2009

Ivo Senjanović
ivo.senjanovic@fsb.hr
Smiljko Rudan
smiljko.rudan@fsb.hr
Nikola Vladimir
nikola.vladimir@fsb.hr
University of Zagreb
Faculty of Mechanical Engineering and
Naval Architecture
I. Lučića 5, 10000 Zagreb, Croatia